PERGAMON

International Journal of Engineering Science 36 (1998) 1035–1046

International Journal of Engineering Science

Some remarks on the acoustic parameters of sharp-edged porous media

M. Firdaouss[a,b], J.-L. Guermond[a,*], D. Lafarge[c]

[a]*LIMSI, UPR-CNRS 3251, BP 133, 91403 Orsay, France*
[b]*UFR 923, UPMC Paris VI, Paris, France*
[c]*LAUM, UMR CNRS 6613, 72085 Le Mans Cedex 9, France*

Received 13 June 1997; accepted 19 October 1997

Abstract

This work revisits some numerical experiments by Smeulders et al. [Smeulders DMJ, Van Hassel RR, Van Dongen MEH, Jansen JK. Int. J. Eng. Sci. 1994;32(6):979]. It concerns the acoustic properties of two-dimensional porous media whose pore surface is rugged. Contrary to what is inferred by Smeulders et al., we discover that Johnson's shape factor, M, remains finite and is in the order of unity if the surface is not cusped. However, in agreement with Smeulders et al., $M \longrightarrow +\infty$ when the pore surface has a sharp edge whose angle tends to zero.

1. Introduction

The propagation of sound in fluid saturated porous media with rigid solid frame is of great interest for a large class of industrial applications. With air as the pore fluid, applications can be found in noise control, non-destructive characterization of materials, thermoacoustically controlled heat transfers, etc. We assume that the pore fluid motions can be described, at the microscopic level, by the compressible Navier–Stokes/Fourier model of linear acoustics [1]. Then, it is possible to build simple effective medium macroscopic models of the acoustic propagation by means of the homogenization theory, provided the length-scale of the sound waves is much larger than the microscopic length-scale of the pores. In particular, if the porous media is assumed to be roughly periodic and the dependence in time to be harmonic, then two macroscopic variables, the mean velocity $\langle v \rangle$ and the mean pressure $\langle p \rangle$ can be related by the dynamic Darcy law:

* Corresponding author. Tel.: +33-1-6985-8069; Fax: +33-1-6985-8088; E-mail: guermond@limsi.fr.

0020-7225/98/$19.00
PII: S0020-7225(98)00002-0

$$\langle v\rangle = -\frac{1}{\phi\eta}k(\omega)\cdot\nabla\langle p\rangle, \tag{1.1}$$

where η is the dynamic viscosity of the fluid, ϕ is the porosity and the symbol $\langle.\rangle$ denotes a spatial average relative to the fluid phase. The macroscopic coefficient $k(\omega)$ accounts for different hidden processes occurring at the pore scale, namely, it contains inertial drag effects and viscous dissipative effects due to the fluid/solid interactions. This coefficient is called the dynamic permeability of the porous medium [2]; it depends on the frequency ω, since the microscopic structure of the fluid flow evolves with it and reduces to the static Darcy permeability k_0 when ω is zero. This coefficient is a priori a tensor, but for the sake of simplicity we shall identify $k(\omega)$ with a scalar, i.e. the porous medium is assumed to be isotropic, or the sound wave to propagate along one principal axis. As mentioned above, Eq. (1.1) is a direct consequence of the simple two-scale homogenization analysis [2]. The latter gives an explicit recipe for calculating $k(\omega)$ from the knowledge of the microstructure: the response factor $k(\omega)$ is the same as that occurring in the *formal* problem of determining the oscillatory flow of an *incompressible* viscous fluid, driven through the porous medium by an applied *uniform* oscillatory pressure gradient [17,18]. Another alternative form of Eq. (1.1) consists in introducing the dynamic tortuosity (identified to a scalar), $\alpha(\omega)$, so that we have

$$-i\omega\rho_f\alpha(\omega)\cdot\langle v\rangle = -\nabla\langle p\rangle, \tag{1.2}$$

where ρ_f is the ambient density of the saturating fluid. To deduce the acoustic properties of the porous medium, a second macroscopic equation that expresses the pressure–density relationship in the fluid is required. In terms of $\langle p\rangle$ and $\langle v\rangle$ this equation reads:

$$-i\omega\frac{1}{K_a}\beta(\omega)\langle p\rangle = -\nabla\cdot\langle v\rangle, \tag{1.3}$$

where K_a is the adiabatic bulk modulus of the pore fluid. The scalar coefficient $\beta(\omega)$ is a scaled dynamic compressibility of the pore fluid, that accounts for possible deviations from the adiabatic pressure–density relationship caused by the thermal exchanges with the solid frame. In the present note we shall restrict ourselves to the dynamic permeability/tortuosity problem. Some information on the modeling of $\beta(\omega)$ can be found elsewhere [3].

An important parameter coming into the characterization of porous media is the high frequency limit of the dynamic tortuosity; hence, it is usual to introduce the following notation:

$$\alpha_\infty = \lim_{\omega\to\infty}\alpha(\omega). \tag{1.4}$$

The tortuosity α_∞ can also be written ϕF where F is Brown's formation factor [4]. Using the low frequency and high frequency parameters k_0 and α_∞, Johnson et al. [5] proposed a simple scaling function for the dynamic tortuosity as follows:

$$\frac{\alpha(\omega)}{\alpha_\infty} = 1+\frac{i}{x}\left[1-iM\frac{x}{2}\right]^{1/2}, \tag{1.5}$$

where x is a dimensionless frequency: $x = \omega k_0 \alpha_\infty \rho_f / \phi\eta$ and M is a dimensionless shape factor defined in 2D by

$$M = \frac{12\alpha_\infty k_0}{\phi \Lambda^2}. \tag{1.6}$$

For three-dimensional flows, the factor 12 should be replaced by 8. The parameter Λ [6] is the sole additional parameter of the model and it has the dimension of a length. This model has been proved to be very robust for a large class of porous media and the shape factor M is usually found to be of order unity. It is suggested in Smeulders et al. [7] that Johnson's model may fail when the pores of the medium have sharp edges, since for this kind of microstructure the shape factor may reach very large values (viz. 10^2 to 10^3).

Smeulders et al. substantiate their claim by considering a two-dimensional periodic canal limited by jaggered walls as depicted in Fig. 1(left). Given the periodicity and the symmetry of the problem, only one fourth of the periodic cell needs to be considered (see Fig. 1(right)). Hereafter, the axial length of the periodic cell is set to 1 and its height is equal to 2; the height of the sharp edge is denoted by h and its width by b. Smeulders et al. [7] have evaluated numerically the coefficient Λ for different values of b and h. More specifically, they considered two classes of test cases: first they performed calculations for $0.1 \leq b = h \leq 0.8$, second they fixed $h = 0.5$ and let b vary within the interval $0.1 \leq b \leq 0.8$. For the first case they found that $M \to \infty$ when $h \to 1$; for instance, they obtained $M = 120$ for $h = 0.8$. For the second case, they found that $M \to \infty$ when $b/h \to 0$; for instance, they obtained $M = 210$ for $b/h = 0.2$ and $h = 0.5$.

In this work we revisit the numerical experiments considered by Smeulders et al. [7]. Quite unexpectedly we do not reach the same conclusions as those reported above. Actually, we discover that M remains finite and is of order unity if $b = h$; that is to say, the shape factor does not vary very much when h varies and the angle of the sharp edge is fixed and different from zero. However, in agreement with the reference above, we obtain that $M \to \infty$ when

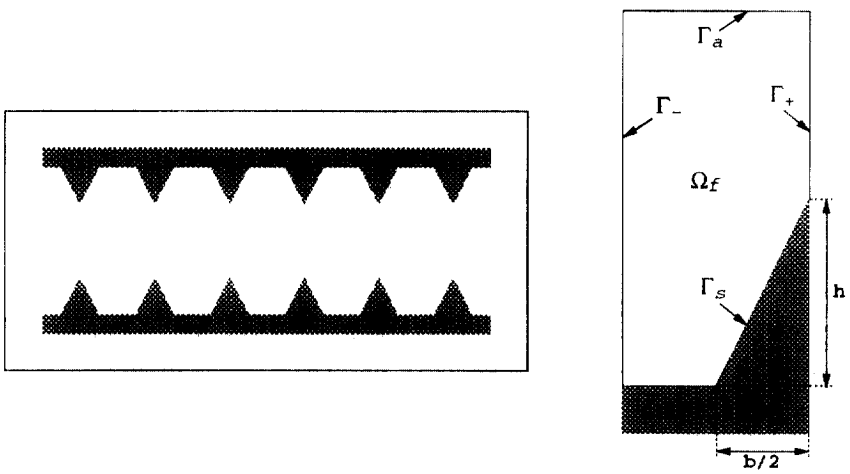

Fig. 1. Geometry of a 2D canal with jaggered walls (left). Geometry of half the periodic cell (right).

$b/h \to 0$ and h is fixed; that is to say, the shape factor diverges when the angle of the sharp edge tends to zero. This is because, as previously shown by Achdou and Avelleneda [8] on the basis of simple potential theory considerations, the parameter Λ must go to zero in presence of sharp edges. Our numerical results are coherent with this finding. In conclusion, the shape factor seems to be controlled more by the angle of the sharp edge than by its height.

This paper is organized as follows. In Section 2 we recall the basic facts concerning the microscopic problems to be solved. Section 3 reports on our numerical results and the conclusions that can be drawn from them.

2. Formulation of the problem

2.1. The microscopic equations

When considering a periodic porous medium, the homogenization theory [9,2], yields an explicit mean to evaluate $\alpha(\omega)$. Let us denote by Ω_0 the cell which repeats itself periodically in the entire porous domain; Ω_0 is the union of Ω_f and Ω_s where Ω_f is the fluid domain and Ω_s is the solid domain; the interface between Ω_f and Ω_s is denoted by Γ_s (see Fig. 1(right)). For any unit vector e of arbitrary direction in space, we consider the following microscopic problem posed in Ω_f: find v and p so that

$$-\frac{i\omega}{\nu} v - \Delta v + \frac{1}{\eta}\nabla p = e, \qquad \nabla \cdot v = 0, \qquad v_{|\Gamma_s} = 0, \qquad v \text{ and } p, \ \Omega_0\text{-periodic}, \tag{2.1}$$

where $\nu = \eta/\rho_f$. Then, many interesting macroscopic properties of the porous media can be deduced from the velocity field v. In particular it can be shown that the dynamic permeability and the tortuosity can be computed explicitly as follows:

$$k(\omega) = \frac{\phi}{|\Omega_f|}\int_{\Omega_f} v(\omega)\cdot e \, d\Omega, \tag{2.2}$$

$$\frac{1}{\alpha(\omega)} = -\frac{i\omega}{\nu|\Omega_f|}\int_{\Omega_f} v(\omega)\cdot e \, d\Omega, \tag{2.3}$$

where $|\Omega_f|$ denotes the volume of Ω_f. Within the two-scale homogenization theory, e is the macroscopic gradient of the macroscopic pressure (see, for example, Refs. [9,2,7] for more details). We hereafter assume that $k(\omega)$ does not depend on the direction of the unit vector e; that is to say, we assume that the porous medium is isotropic.

Although the microscopic problem is valid for all values of ω (note however that within the homogenization theory the wavelength must be larger than the microscopic cell length-scale) it is not convenient to solve it when $\omega \to \infty$ since in this limit boundary layers appear. Hence, when considering the high frequency behavior of the solution it is preferable, for computational purposes, to solve directly the degenerate problem:

$$E + \nabla\psi = e, \qquad \nabla \cdot E = 0, \qquad E \cdot n_{|\Gamma_s} = 0, \qquad E \text{ and } \psi, \ \Omega_0\text{-periodic}. \tag{2.4}$$

It can be shown (see, for example, Refs. [10, 5]) that α_∞ and Λ derive directly from the vector field E by means of

$$\alpha_\infty = \frac{|\Omega_f|}{\int_{\Omega_f} E^2 \, d\Omega}. \tag{2.5}$$

$$\Lambda = \frac{2\int_{\Omega_f} E^2 \, d\Omega}{\int_{\Gamma_s} E^2 \, d\Gamma} \tag{2.6}$$

In conclusion, the homogenization theory provides us with a mean to test Johnson's formula by applying it on model periodic porous media. In particular we can evaluate the shape factor M on model problems by calculating k_0, α_∞ and Λ by means of the formulae given above.

2.2. On the singular behavior of E

When Γ_s is smooth, it can be shown that ψ is smooth and accurate numerical approximations of E can be obtained routinely. However, if Ω_f has a sharp edge, then ψ is not smooth in the vicinity of the singularity of Γ_s and E, being a function of the gradient of ψ, may be very singular. Let us illustrate this point in 2D. Assume that Γ_s has a sharp edge in the vicinity of O and denote by $\gamma\pi$ the interior angle of the wedge; then, the standard potential theory shows that ψ behaves in the vicinity of O as follows:

$$\psi \approx r^{1/(2-\gamma)} \cos(\theta/(2-\gamma)), \tag{2.7}$$

where (r, θ) denote the cylindrical coordinates with the origin in O and the fluid domain is identified to $]0, +\infty[\times]0, (2-\gamma)\pi[$. As a result, the trace of E^2 on Γ_s behaves like

$$E_{|\Gamma_s} \approx r^{-1+\gamma/(2-\gamma)}. \tag{2.8}$$

When γ tends to zero, the exponent of the singularity of E^2 converges to -1; since this singularity is not integrable, Λ is necessarily zero when Γ_s is cusped. This phenomenon is in part at the origin of the interests of investigators for sharp-edged porous media, since for this class of cell geometry the shape factor M is infinite according to Eqs. (1.6), (2.1), (2.2), (2.3), (2.4), (2.5) and (2.6). However, from the numerical point of view, the computation of the surface integral in Eq. (2.6) is quite difficult in practice if Γ_s has sharp edges. For instance, if $\gamma\pi$ is equal to $\pi/6$ (which is a moderately sharp angle), the exponent of the singularity of E^2 is of order -0.91. As a result, if no particular care is given to the computation of E^2 and its integral, then very large numerical errors are likely to occur. To convince himself, the reader may try to compute $\int_0^1 dx/x^{0.91}$ by means of the Simpson rule on a uniform grid. Hence, the computation of ψ and E^2 needs to be very accurate in the vicinity of the sharp edge to avoid very large errors. The numerical strategy that we have adopted to ensure high accuracy in our computation is presented in Section 3.

3. Numerical results

3.1. The finite element procedure

Eq. (2.4) can alternatively be written in the form

$$\Delta\psi = 0, \qquad \frac{\partial\psi}{\partial n_{|\Gamma_s}} = e \cdot n_{|\Gamma_s}, \quad \psi \text{ periodic}; \qquad E = e - \nabla\psi. \tag{3.1}$$

The scalar field ψ is solution to a classical elliptic problem. Given the symmetries of the problem, it is possible to restrict the computational domain to one fourth of the periodic cell as depicted in Fig. 1(right). Let Γ_-, Γ_a, Γ_+ and Γ_s denote the pieces of the boundary of the fluid domain Ω_f as shown in Fig. 1(right). Then, setting $e = (1, 0) = \nabla x$ for the sake of simplicity and defining Ψ by $\Psi = x - \psi$, Eq. (3.1) can be put into the simple form

$$\Delta\Psi = 0, \qquad \frac{\partial\Psi}{\partial n_{|\Gamma_s \cup \Gamma_a}} = 0. \qquad \Psi_{|\Gamma_-} = 0.5, \qquad \Psi_{|\Gamma_+} = 0, \qquad E = \nabla\Psi. \tag{3.2}$$

Hereafter, we approximate the solution to Eq. (3.2) by means of P_1 finite elements and by using the variational formulation of the problem. To ensure that the solution is very accurately calculated, we have used an iterative automatic adaptive refinement method. More precisely, the solution is calculated on a given P_1 mesh, then an a posteriori estimate of the error is calculated, finally the mesh is refined accordingly by means of a Delaunay technique devised by Rebay [11]. The procedure is repeated until the norm of the a posteriori error estimate reaches a prescribed level. The whole procedure has been tested on singular problems and has proved to be very effective. The performance of the finite element solver that is used to carry out the computation is reported in [12]. To give an idea of the meshes that have been used, we plot in Fig. 2 the mesh corresponding to the domain $b = 0.4$, $h = 0.5$, together with a close up of the sharp edge region.

To make sure that the potential, ψ, together with its tangential derivative is correctly evaluated, we have systematically verified that in the vicinity of the sharp edge the numerical potential behaves as follows

$$\psi = A_1 r^{\beta} + A_2 r^{3\beta} + o(r^{3\beta}), \tag{3.3}$$

where $\beta = 1/(2-\gamma)$ and r is the distance from the wedge tip. This behavior is inferred from the classical potential theory. For the particular case $h = 0.5$ and $b = 0.5$, we have plotted on Fig. 3 ψ/s^{β} as a function of s, where s is the curvilinear abscissa along the solid boundary, the origin being set at the extremity of the sharp edge. This test clearly demonstrates that the numerical solution behaves asymptotically like $A_1 s^{\beta}$ when s tends to zero. On Fig. 3 we have also plotted $(\psi - A_1 s^{\beta})/s^{3\beta}$ as a function of s, where the coefficient A_1 is the numerical limit of the ratio ψ/s^{β} when s tends to zero. Fig. 3 shows that our numerical calculation behaves asymptotically correctly up to the second order term in the vicinity of the sharp edge.

To avoid large numerical errors induced by numerical derivation with respect to s in the vicinity of the sharp edge, we have adopted the following mixed strategy to compute the integral $\int_{\Gamma_s} E^2 \, d\Gamma$. In a small vicinity of the sharp edge, say $0 \le s \le s_0$, we replace the numerical

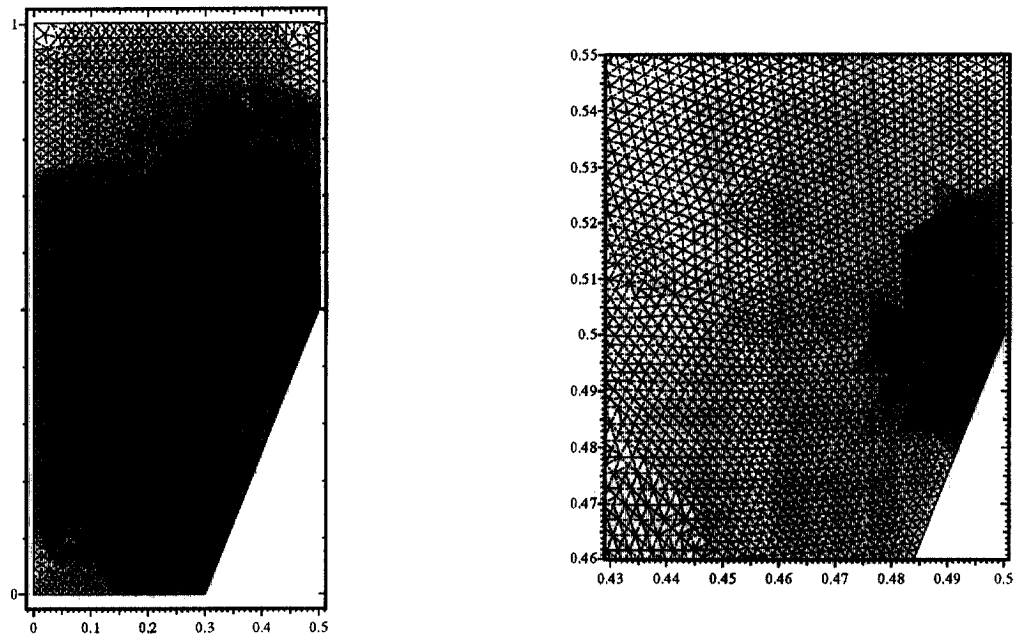

Fig. 2. Left: P1 mesh corresponding to domain $b = 0.4$, $h = 0.5$. Right: close up of the sharp edge region.

solution by its asymptotic behavior (Eq. (3.3)) up to the second order term, where A_1 and A_2 are obtained by interpolation. Then we evaluate $E = \partial(x - \psi)/\partial_s$ in the interval $0 < s < s_0$, by derivating Eq. (3.3) with respect to s and the integral $\int_0^{s_0} E^2 \, ds$ is calculated analytically. For s larger than s_0, we evaluate the approximate derivative by means of a spline fitting and the

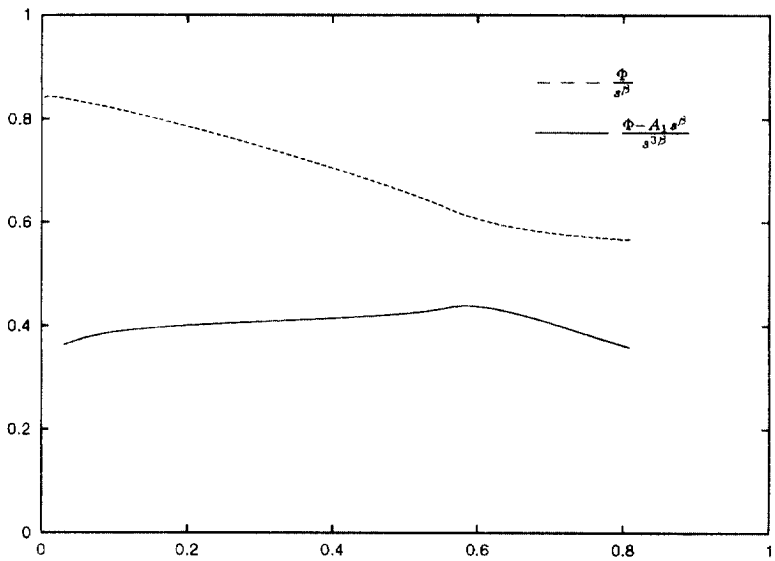

Fig. 3. Asymptotic behavior of ψ for the case $b = 0.5$, $h = 0.5$.

Table 1
Numerical results for case $h = 0.5$

b	0.1	0.2	0.3	0.4	0.5	0.6	0.7	0.8	0.9
k_0	0.0705	0.0703	0.0702	0.0701	0.0699	0.0697	0.0694	0.0691	0.0687
α_∞	1.389	1.365	1.342	1.319	1.296	1.272	1.249	1.224	1.199
Λ	0.151	0.288	0.412	0.516	0.616	0.693	0.765	0.822	0.870
M	53.1	14.6	7.19	4.62	3.27	2.61	2.15	1.88	1.69

integral is approximated by means of a compound Simpson rule. Typically, s_0 varies between 1 to 5% of the total length of Γ_s.

3.2. Angle of the sharp edge is variable

In this section we report on the results that we have obtained on the test cases defined in Smeulders et al. [7]. We consider a canal with a sharp edge of fixed height h and we choose b, the width at its base, as a parameter. We have explored the interval $0.1 \leq b \leq 0.9$ with $h = 0.5$ (Table 1). The Johnson length, Λ, is plotted in Fig. 4. The dashed line corresponds to the results obtained by the present calculations, whereas the solid line represents the results reported in Ref. [7]. The disagreement between the two sets of results is evident. The ratio of Λ obtained by the present method to that from Ref. [7] varies between 2.0 and 2.5. Note that to compute Λ, the value of α_∞ is required; this quantity is evaluated by calculating $\int_{\Omega_f} E^2 \, d\Omega$ and by using Eq. (2.5). In every case that we have computed, the value of α_∞ obtained by the present calculations was in agreement with that given in Ref. [7] up to the third or fourth digit. Hence, the only difference that exists between the present calculation and that reported in Ref. [7] lies in the evaluation of the surface integral $\int_{\Gamma_f} E^2 \, d\Omega$.

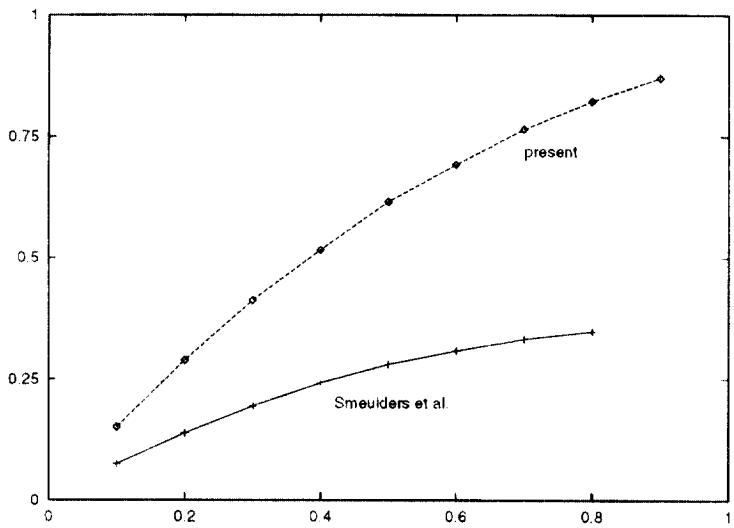

Fig. 4. Λ as a function of b ($0.1 \leq b \leq 0.9$) for $h = 0.5$. The dashed line represents the finite element calculations, whereas the solid one represents the results from Ref. [7].

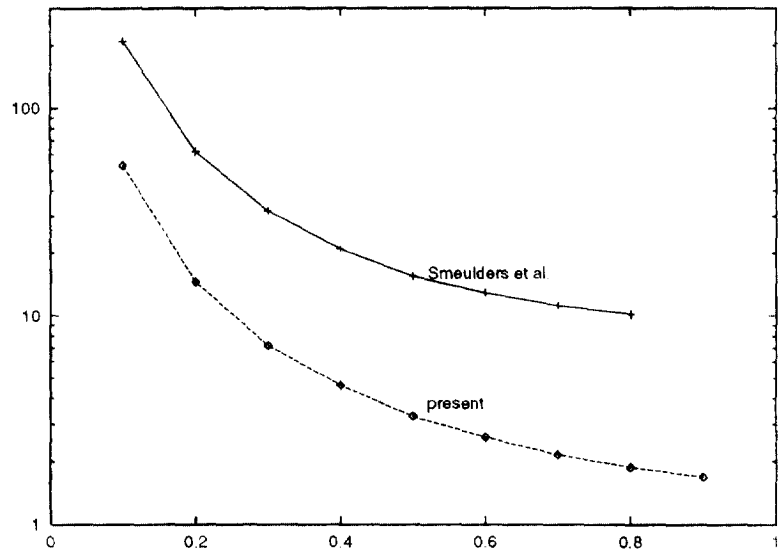

Fig. 5. Coefficient M as a function of b ($0.1 \leq b \leq 0.9$) for $h = 0.5$. The dashed line represents the finite element calculations, whereas the solid one represents the results from Ref. [7].

The shape factor M introduced by Johnson is calculated by using Eq. (1.6), where the static permeability, k_0, is evaluated by solving Eq. (2.1) for $\omega = 0$ and by using Eq. (2.2). The value of k_0 obtained by the present calculation is in agreement with that given in [13, 7] up to the third or fourth digit in every case tested. The shape factor, M, as a function of b is plotted in Fig. 5. The dashed line corresponds to the results obtained by the present calculation, whereas the solid line represents the results given by Ref. [7]. The disagreement between the two sets of results is even worse than before since M is inversely proportional to Λ^2. The ratio of M calculated by the present method to that given by Ref. [7] varies between 4.0 and 6.0. Note however, that the conclusion of Ref. [7] still holds; that is to say, the shape factor tends to infinity when the interior angle $\gamma\pi$ of the sharp edge tends to zero. As a result, Johnson's model may not be suitable for approximating the behavior of porous media having cusped pore surface. This will be verified in a forthcoming paper.

3.3. Angle of the sharp edge is constant

We consider in this section a canal with a sharp edge whose height h is equal to the base width, b (Table 2). The computations have been carried out for $0.01 \leq b = h \leq 0.988$. In Fig. 6 we have plotted Λ as a function of b. The results obtained by the present calculations are plotted in dashed line and those coming from Ref. [7] are in solid line. The two sets of results are clearly different. The ratio of the value of Λ calculated by the present method to that from Ref. [7] varies between 1.0 to 5.0. Note however that the value of α_∞ obtained by the present calculation was in agreement with that given in Ref. [7] up to the third or fourth digit. Once again, the large differences that exist between the present calculation and that reported in Ref. [7] come from the computation of the surface integral $\int_{\Gamma_f} E^2 \, d\Omega$.

Table 2
Numerical results for case $h = b$

b	0.01	0.1	0.2	0.3	0.4	0.5	0.6	0.7	0.8
k_0	0.331	0.299	0.232	0.165	0.110	0.070	0.0407	0.0210	8.63×10^{-3}
α_∞	1.000	1.013	1.051	1.112	1.194	1.296	1.422	1.584	1.815
Λ	1.915	1.373	1.047	0.885	0.728	0.616	0.525	0.423	0.325
M	1.08	1.94	2.72	3.15	3.24	3.27	3.07	2.94	2.62

b	0.9	0.92	0.94	0.96	0.98	0.988
k_0	2.09×10^{-3}	1.35×10^{-3}	7.71×10^{-4}	3.59×10^{-4}	9.07×10^{-5}	3.63×10^{-5}
α_∞	2.233	2.376	2.568	2.853	3.365	3.752
Λ	0.207	0.177	0.146	0.111	0.066	0.046
M	2.24	2.13	2.01	1.86	1.61	1.55

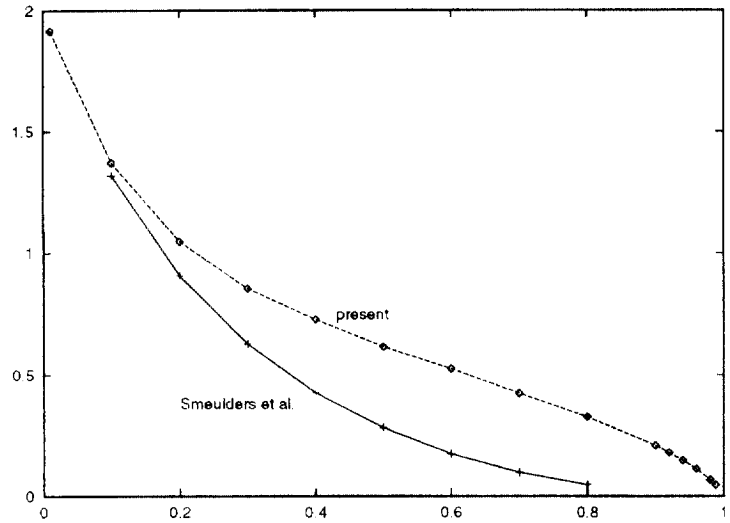

Fig. 6. Λ as a function of b ($0.01 \leq b = h \leq 0.988$) for the case $h = b$. The dashed line represents the finite element calculations, whereas the solid one represents the results rom Ref. [7].

In Fig. 7 the shape factor, M, is plotted as a function of b. The present calculations are plotted in dashed line and the solid line represents the results from Ref. [7]. The disagreement between the two sets of results is clear; they even show different asymptotic behavior as h tends to 1. The shape factor obtained by the present finite element technique seems to converge very slowly to zero as h tends to 1, i.e. the pore throat tends to zero, whereas the values given in

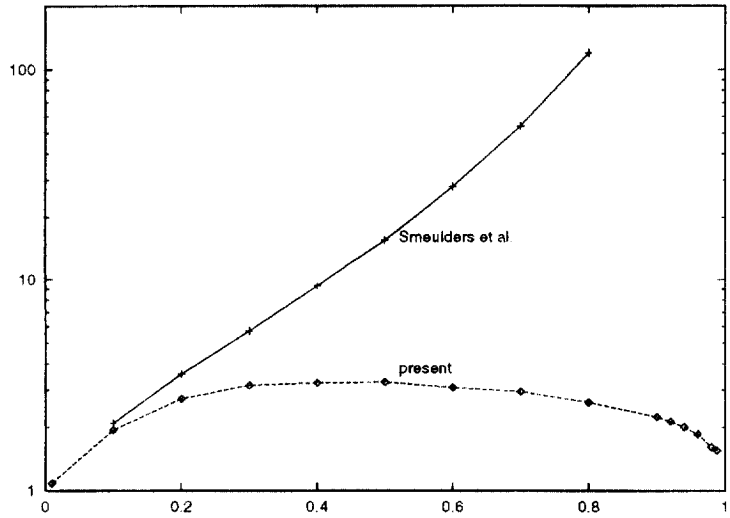

Fig. 7. Coefficient M as a function of b ($0.01 \leq b = h \leq 0.9880$ for the case $h = b$. The dashed line represents the finite element calculations, whereas the solid one represents the results from Ref. [7].

Ref. [7] seems to diverge to infinity (for instance $M(0.8) = 120$). As a result, the present calculations show that for a constant value of the angle $\gamma\pi$, the shape factor is weakly dependent on h; in the present case the value of M varies between 1 and 3. Such values also seem in agreement with a number of different numerical estimates recently made for different geometries [8, 5, 14–16, 13]. This tends to show that for porous media whose pore surface is rugged but not cusped, Johnson's model is uniformly valid, in a first approximation, throughout the entire frequency range. The extent to which this is indeed the case will be investigated in the mentioned forthcoming paper.

References

[1] Pierce AD. Acoustics, An introduction to its physical principles and applications. New-York: McGraw-Hill, 1981.
[2] Levy T, Sanchez-Palencia E. J Math Anal Appl 1977;61(3):813.
[3] Lafarge D, Lemarinier P, Allard J-F, Tarnow V. J Acoust Soc Am;1997, submitted.
[4] Brown R. Geophysics 1980;45:1269.
[5] Johnson DL, Koplik J, Dashen R. J Fluid Mech 1987;176:379.
[6] Johnson DL, Koplik J, Schwartz LM. Phys Rev Lett 1986;57:2564.
[7] Smeulders DMJ, Van Hassel RR, Van Dongen MEH, Jansen JK. Int J Eng Sci 1994;32(6):979.
[8] Achdou Y, Avellaneda M. Phys Fluids A 1992;4:2651.
[9] Auriault JL. Int J Eng Sci 1980;18:775.
[10] Avellaneda M, Torquato S. Phys Fluids A 1991;3(11):2529.
[11] Rebay S. J Comput Phys 1993;106:125.
[12] Guermond J-L, Quartapelle L. J Comput Phys 1997;132:1.
[13] Smeulders DMJ, Eggels RL, Van Dongen ME. J Fluid Mech 1992;245:211.
[14] Kostek S, Schwartz LM, Johnson DL. Phys Rev B 1992;45:186.
[15] Pride SR, Morgan FD, Gangi AF. Phys Rev B 1993;47:4964.
[16] Saeger RB, Scriven LE, Davis HT. Phys Rev A 1991;44:5087.
[17] Sheng P, Zhou MY. Phys Rev Lett 1988;61:1591.
[18] Zhou MY, Sheng P. Phys Rev B 1989;35:12027.